



ROYAL  
HOLLOWAY  
UNIVERSITY  
OF LONDON

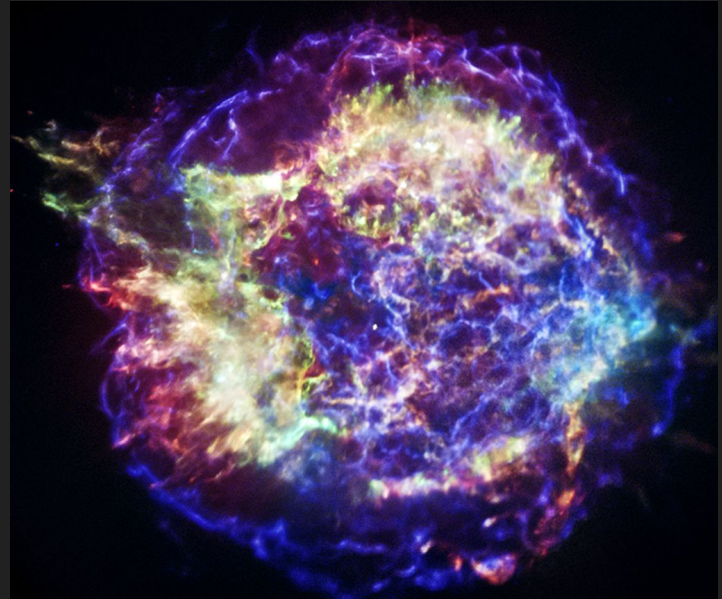
STFC Intro to Astro Summer School  
4 September 2025

# Machine learning approaches to radio astronomy

**Dr. Vanessa Gruber**

**UKRI Future Leaders Fellow**

**Royal Holloway, University of London**



Cassiopeia A supernova remnant  
(credit: NASA/CXC/SAO)



ROYAL  
HOLLOWAY  
UNIVERSITY  
OF LONDON

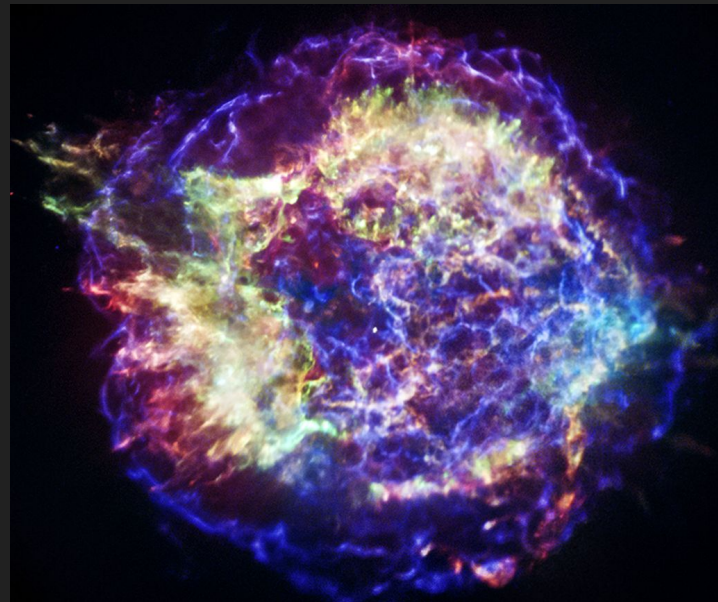
STFC Intro to Astro Summer School  
4 September 2025

# ML approaches to radio astronomy - or how to better understand neutron stars

Dr. Vanessa Graber

UKRI Future Leaders Fellow

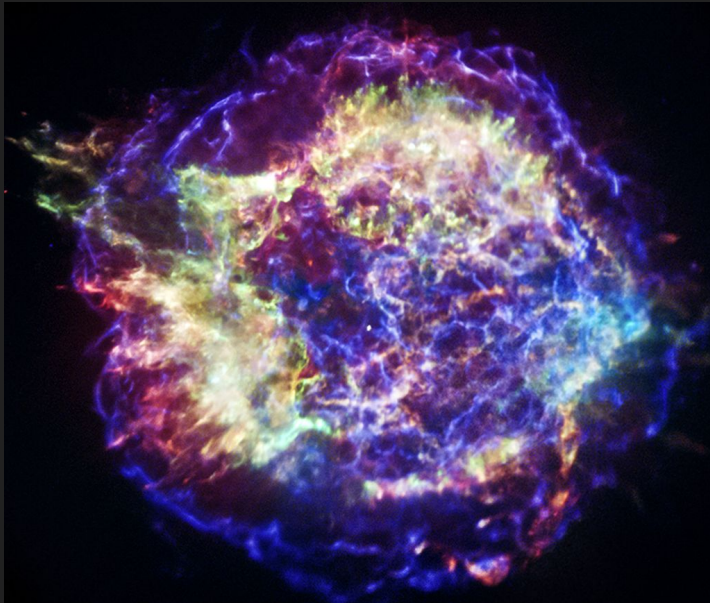
Royal Holloway, University of London



Cassiopeia A supernova remnant  
(credit: NASA/CXC/SAO)

# Outline

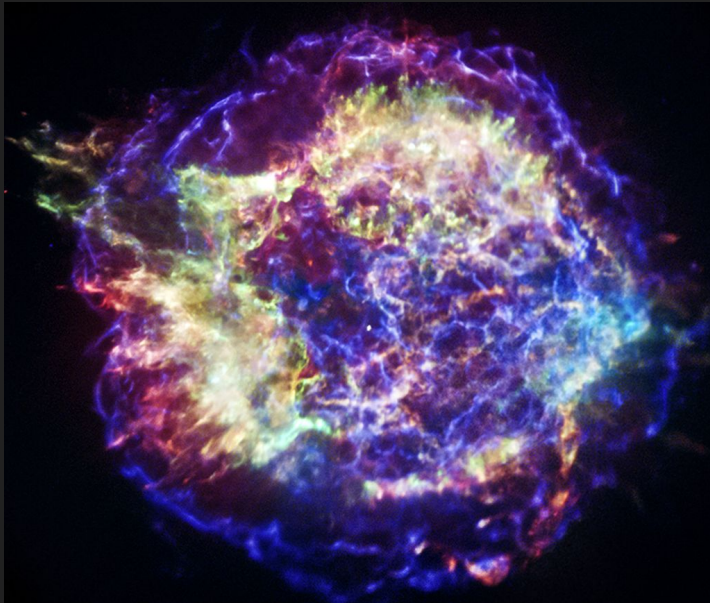
- **Radio Astronomy**
- **ML and Radio Astronomy**
- **Neutron Stars**
- **SBI for Pulsar Populations**
- **Summary**



Cassiopeia A supernova remnant  
(credit: NASA/CXC/SAO)

# Outline

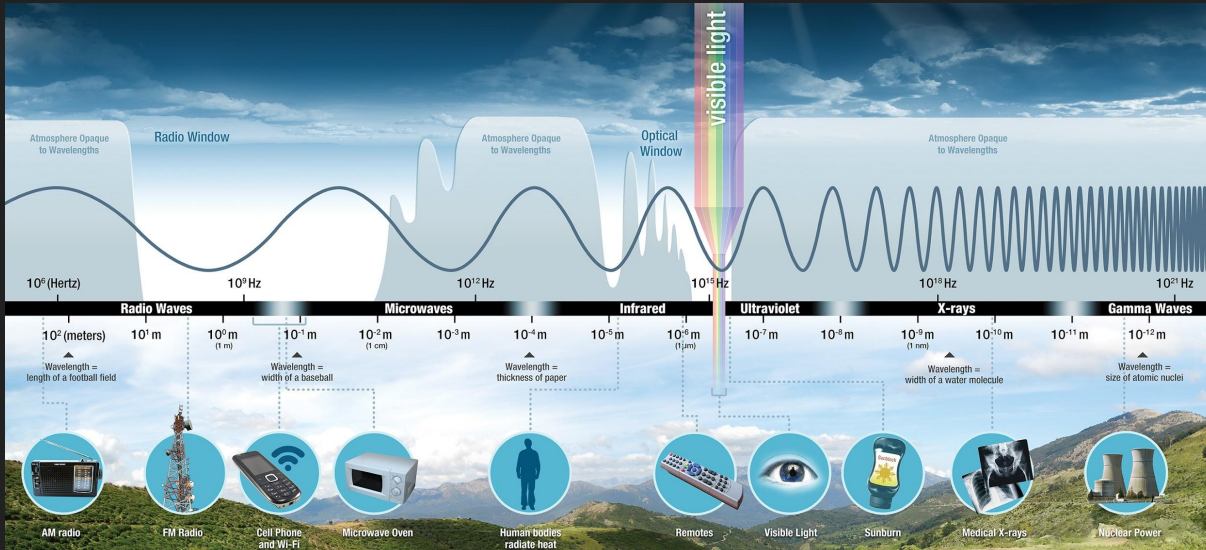
- **Radio Astronomy**
- **ML and Radio Astronomy**
- **Neutron Stars**
- **SBI for Pulsar Populations**
- **Summary**



Cassiopeia A supernova remnant  
(credit: NASA/CXC/SAO)

# The radio window

- Radio astronomy observes the Sky over **many orders of magnitude** from  $\sim 10$  MHz (10m) to  $\sim 1$  THz (1mm) at the low-frequency end of the EM spectrum.

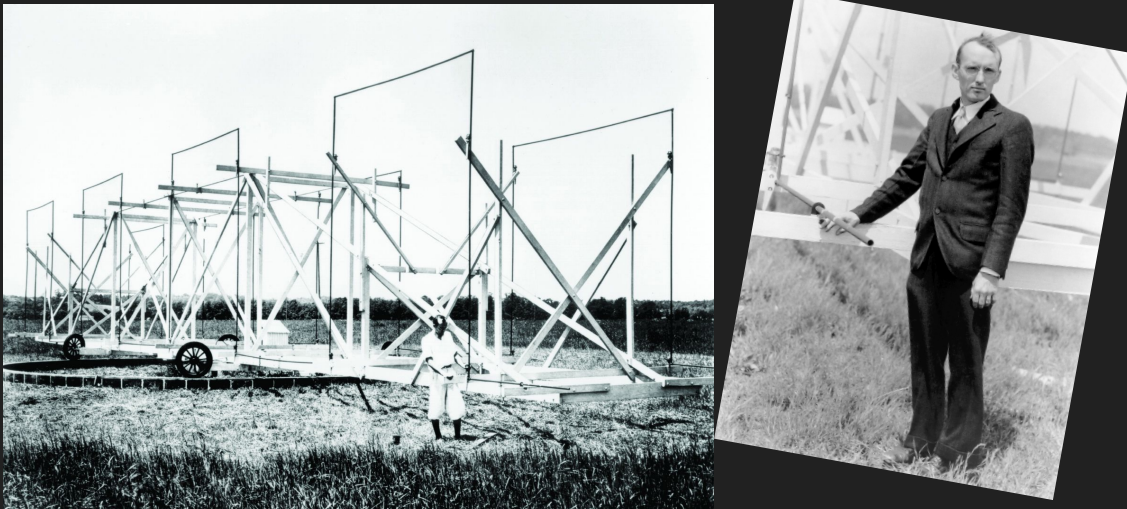


EM spectrum and atmospheric opaqueness. Credit: NASA

- As the Earth's atmosphere is transparent to radio waves, we perform radio astronomy from Earth's surface.
- Since the 1930's, radio astronomers have been given access to an often **hidden Universe**.

# The radio window

- Radio astronomy observes the Sky over **many orders of magnitude** from  $\sim 10$  MHz (10m) to  $\sim 1$  THz (1mm) at the low-frequency end of the EM spectrum.



Karl Jansky and his rotating radio antenna. Credit: NRAO/AUI/NSF

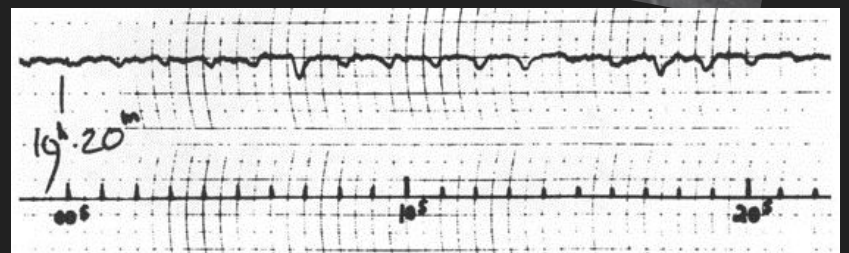
- As the Earth's atmosphere is transparent to radio waves, we perform radio astronomy from Earth's surface.
- Since the 1930's, radio astronomers have been given access to an often **hidden Universe**.

# Science in the radio band I

- Nearly everything in the Universe (e.g., stars, planets, galaxies, clouds of dust, gas molecules and the CMB) emits radio waves due to a variety of emission processes.
- Because radio waves can penetrate dust and gas, many sources that are invisible at other wavelengths can be observed at radio frequencies.
- Radio astronomy has led to many major discoveries such as neutron stars and Fast Radio Bursts (FRBs).



Pulsar lighthouse radiation.  
Credit: J. Christiansen



Jocelyn Bell Burnell and the first pulsar discovery. Credit: Martin Burnell/NRAO

# Science in the radio band II

- Today, radio astronomy covers an incredible breadth of science from the smallest (solar system) to the largest (cosmological) astronomical scales.



The different Science Working Groups of the Square Kilometre Array Observatory. Credit: SKAO

# Radio observatories

- Every radio telescope is essentially an antenna with a receiver. The shape and size depend on the frequencies and objects we want to observe.

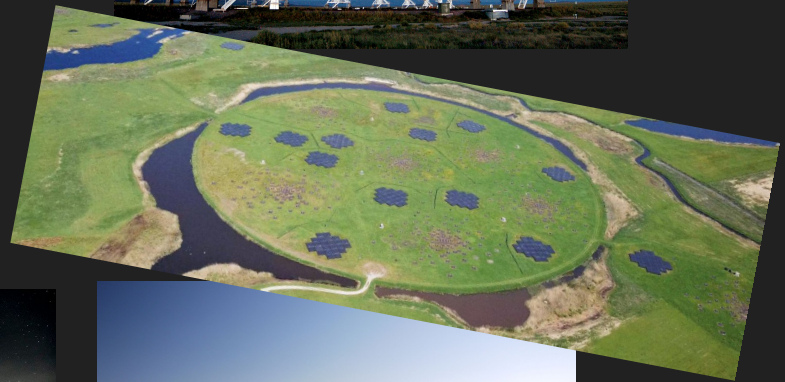


Arecibo. Credit: H. Schweiker/  
WIYN/NOAO/AURA/NSF

CHIME. Credit:  
CHIME  
Collaboration



LOFAR.  
Credit:  
ASTRON



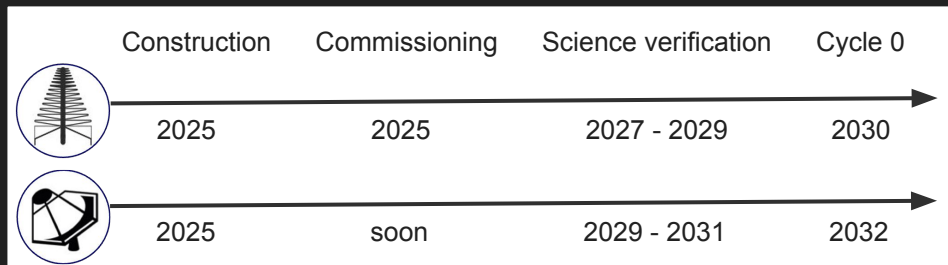
MWA. Credit:  
N. Hurley-  
Walker



Very Large  
Array (VLA).  
Credit:  
NRAO

# Square Kilometre Array Observatory

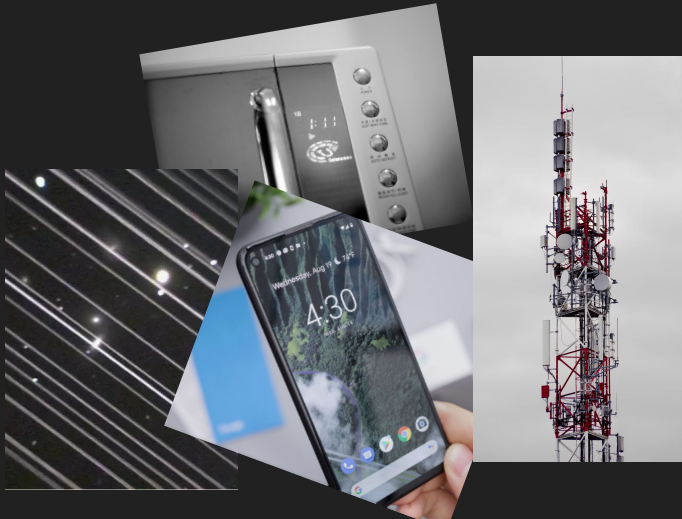
- After many decades of planning, the radio community is (finally) seeing the construction of the Square Kilometre Array Observatory (SKAO).
- Headquartered at Jodrell Bank, SKAO is an intergovernmental organisation to build and operate the world's two largest radio telescopes.



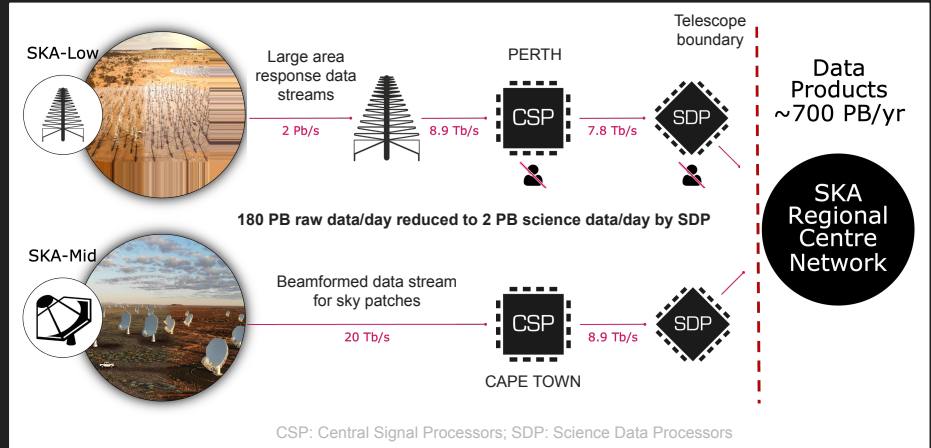
SKA-Mid telescopes in South Africa and SKA-Low stations in Australia. Credit: SKAO

# Challenges in radio astronomy

- Radio astronomy is generally facing two major challenges: radio frequency interference (RFI) and huge data volumes that cannot be analysed by hand.



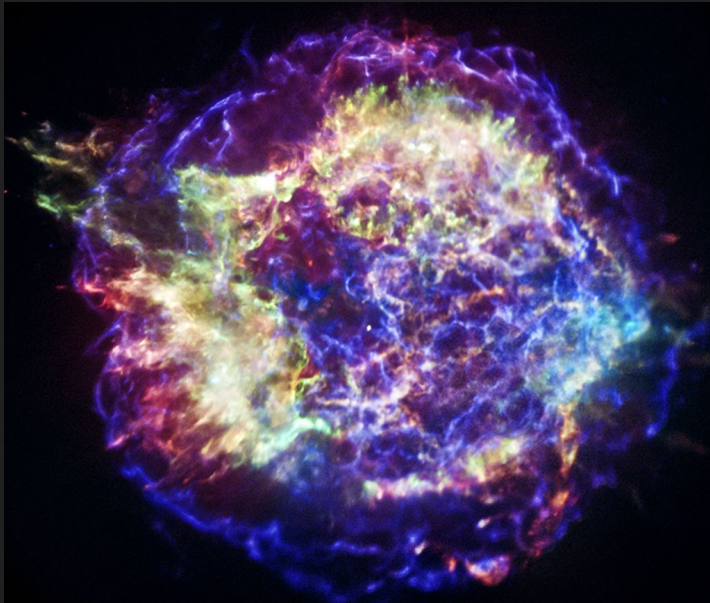
Picking out astronomical signals amongst human made radio signals, instrument noise, etc. is very difficult.



Radio telescopes produce vast amounts of data that need to be sifted and distributed to the end users. Adapted from SKAO.

# Outline

- **Radio Astronomy**
- **ML in Radio Astronomy**
- **Neutron Stars**
- **SBI for Pulsar Populations**
- **Summary**



Cassiopeia A supernova remnant  
(credit: NASA/CXC/SAO)

# Machine learning

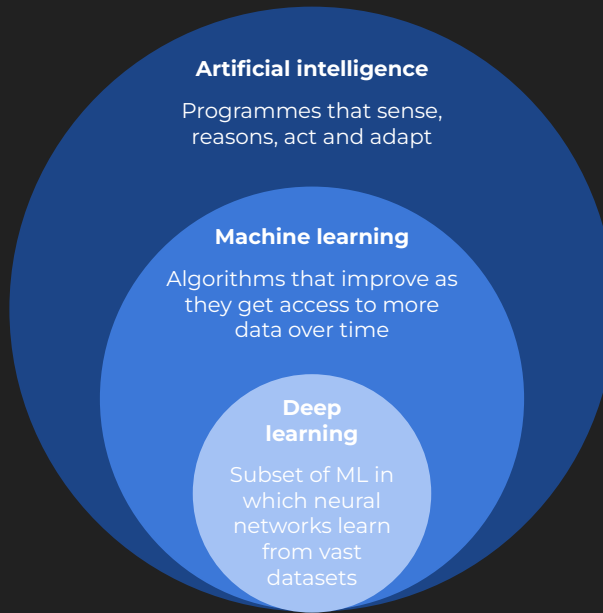
- Several aspects of machine learning (ML) are relevant for radio astronomy:

**Scalability to huge datasets**

**Pattern recognition in complex data**

**Ability to generalise to unknown data**

**Flexible across different domains**



**Real-time processing and decision making**

**Automation and increased efficiency**

**Better accuracy than humans (under certain conditions)**

# Some very recent examples

- The application range of ML for radio astronomy has increased massively in the past 5 years. A few recent examples from the arXiv include:

arXiv:2507.21270 [pdf, ps, other] astro-ph.IM cs.LG

Generative imaging for radio interferometry with fast uncertainty quantification

Authors: Matthijs Mars, Tobias I. Liaudat, Jessica J. Whitney, Marta M. Betcke, Jason D. McEwen

arXiv:2504.09796 [pdf, other] cs.NE astro-ph.IM

Advancing RFI-Detection in Radio Astronomy with Liquid State Machines

Authors: Nicholas J Pritchard, Andreas Wicenec, Mohammed Bennamoun, Richard Dodson

arXiv:2506.11715 [pdf, ps, other] astro-ph.IM doi 10.1051/0004-6361/202554794

Simulating realistic radio continuum survey maps with diffusion models

Authors: Tobias Vičánek Martínez, Henrik W. Edler, Marcus Brüggen

arXiv:2411.15559 [pdf, other] astro-ph.GA doi 10.1093/mnras/staf467

Radio Halo Detection in MWA Data using Deep Neural Networks and Generative Data Augmentation

Authors: Ashutosh K. Mishra, Emma Tolley, Shreyam Parth Kri... Paul Kneib

arXiv:2506.16138 [pdf, ps, other] astro-ph.IM

Radio Galaxy Zoo: EMU -- paving the way for EMU cataloging using AI and citizen science

Authors: Hongming Tang, Eleni Vardoulaki, RGZ EMU collaboration

arXiv:2508.01596 [pdf, ps, other] astro-ph.GA

Identifying Radio Active Galactic Nuclei with Machine Learning and Large-Area Surveys

Authors: Xu-Liang Fan, Jie Li



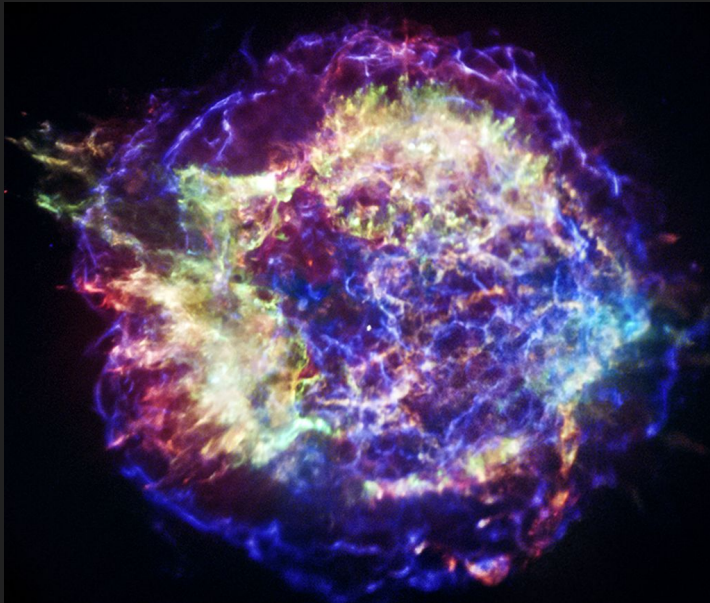
# ML applications for radio astronomy

- ML algorithms have been, e.g., applied to the following types of topics:
  - Telescope optimisation to make the best use of limited resources and manage competing interests.
  - Real-time processing to reduce massive data volumes.
  - Interference mitigation, e.g., via RFI classification or noise reduction to improve data quality.
  - Improve imaging quality for interferometric techniques across multiple telescopes.
  - Source finding and automated classification of millions of sources into different classes to build catalogues (potentially combined with citizen science).
  - Discovery of rare and/or new transient events in real time and efficient follow-up of these phenomena.
  - **Learn more about radio sources to better understand their unknown properties & drive scientific discovery.**



# Outline

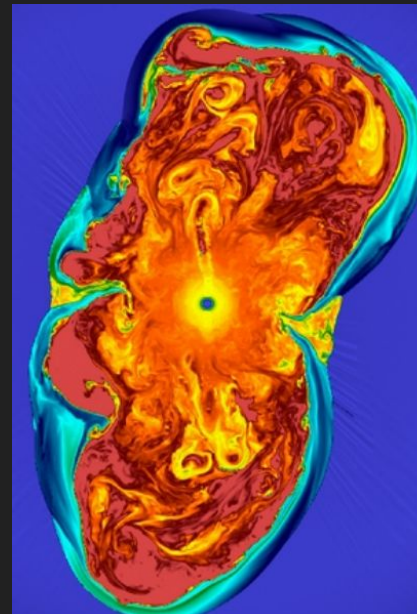
- **Radio Astronomy**
- **ML in Radio Astronomy**
- **Neutron Stars**
- **SBI for Pulsar Populations**
- **Summary**



Cassiopeia A supernova remnant  
(credit: NASA/CXC/SAO)

# Neutron-star formation

- Neutron stars are one of three types of **compact remnants**, created during the **final stages of stellar evolution**.
- When a **massive star of 8 - 25 solar masses** runs out of fuel, it collapses under its own gravitational attraction and **explodes in a supernova**.
- During the collapse, **electron capture** processes ( $p + e^- \rightarrow n + \nu_e$ ) produce (a lot of) neutrons.



**mass:**  $1.2 - 2.1 M_{\odot}$

**radius:** 9 - 15 km

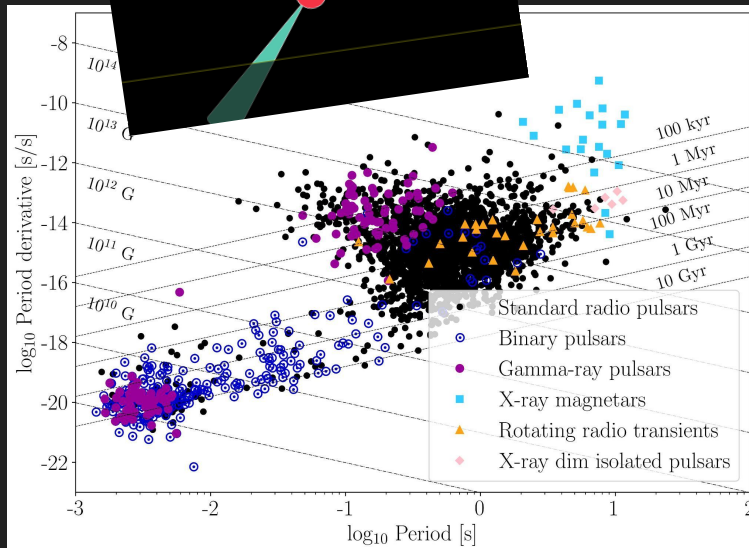
**density:**  $10^{15} \text{ g/cm}^3$

**B-field:**  $10^9 - 10^{15} \text{ G}$

**rotation:**  
10ms - 10s

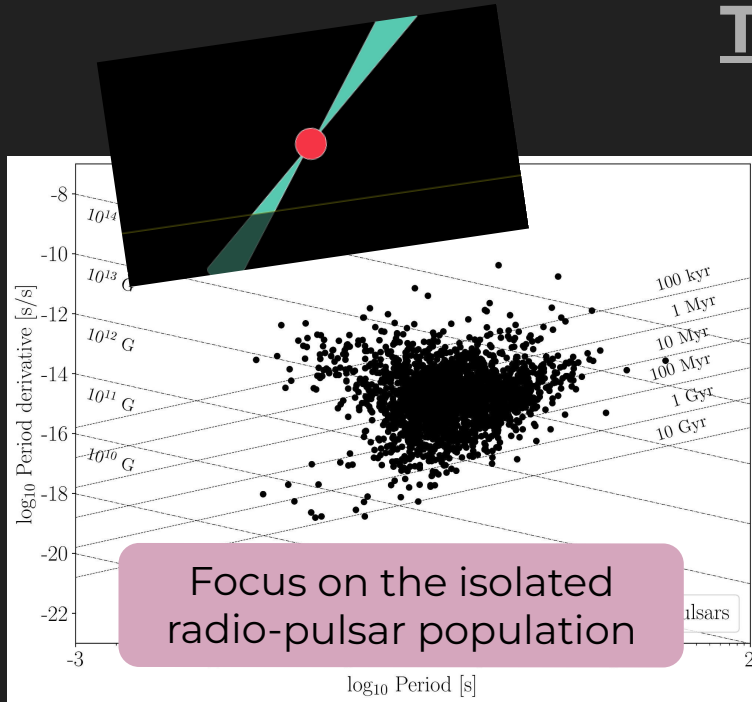
Snapshot of a 3D core-collapse supernova simulation (Mösta et al., 2014)

# The neutron-star zoo



- Pulsars are **very precise clocks** and we time their pulses to **measure rotation periods  $P$  and derivatives  $\dot{P}$** .
  - We now observe neutron stars as pulsars **across the electromagnetic spectrum**.
- ~ **3,500 pulsars** are known to date
- Grouping neutron stars in the  **$P\dot{P}$ -plane** according to their observed properties serves as a diagnostic tool to **identify different neutron-star classes**.

# The neutron-star zoo



Period period-derivative plane for the pulsar population. Data taken from the ATNF Pulsar Catalogue (Manchester et al., 2005)

- Pulsars are **very precise clocks** and we time their pulses to **measure rotation periods  $P$  and derivatives  $\dot{P}$** .
- We now observe neutron stars as pulsars **across the electromagnetic spectrum**.

~ **3,500 pulsars** are known to date

- Grouping neutron stars in the  **$P\dot{P}$ -plane** according to their observed properties serves as a diagnostic tool to **identify different neutron-star classes**.

# Population synthesis: general idea

- We can estimate the **total number of neutron stars in our Galaxy**

$$\text{CC supernova rate: } \sim 2 \text{ per century} \times \text{Galaxy age: } \sim 13.6 \text{ billion years} = \text{NS number: } \sim 2.8 \times 10^8$$

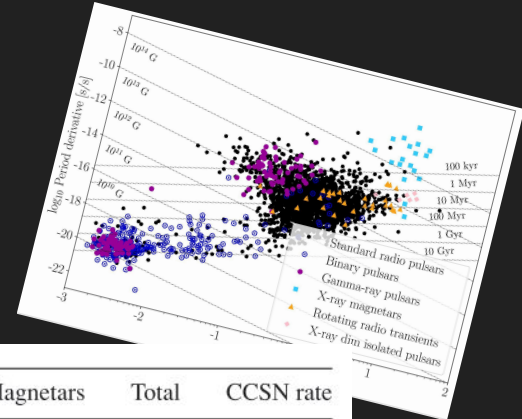
- We only **detect** a very **small fraction** of all neutron stars. Population synthesis bridges this gap focusing on the full population of neutron stars (e.g. Faucher-Giguère & Kaspi 2006, Lorimer et al. 2006, Gullón et al. 2014, Cieślar et al. 2020):



# Goals

- Population synthesis allows us to **constrain the natal properties** of neutron stars and their **birth rates**.
- This is for example **relevant for**:
  - Massive star evolution
  - Gamma-ray bursts
  - Fast-radio bursts
  - Peculiar supernovae
- We can also learn about **evolutionary links between different neutron-star classes** (e.g., Viganó et al., 2013). This is important because estimates for the **Galactic core-collapse supernova rate** are **insufficient** for to explain the independent formation of different classes of pulsars (Keane & Kramer, 2008).

Estimated Galactic core-collapse supernova rate and birth rates for different pulsar classes (Keane & Kramer, 2008).

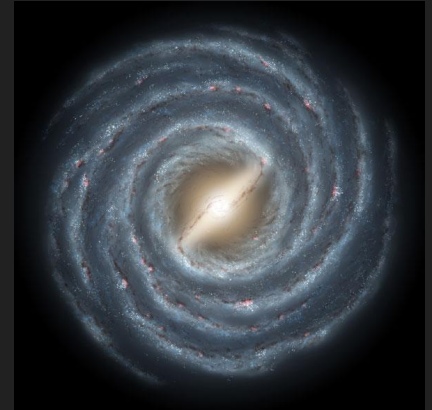


PSRs	RRATs	XDINSS	Magnetars	Total	CCSN rate
$2.8 \pm 0.5$	$5.6^{+4.3}_{-3.3}$	$2.1 \pm 1.0$	$0.3^{+1.2}_{-0.2}$	$10.8^{+7.0}_{-5.0}$	$1.9 \pm 1.1$
$1.4 \pm 0.2$	$2.8^{+1.6}_{-1.6}$	$2.1 \pm 1.0$	$0.3^{+1.2}_{-0.2}$	$6.6^{+4.0}_{-3.0}$	$1.9 \pm 1.1$
$1.1 \pm 0.2$	$2.2^{+1.7}_{-1.3}$	$2.1 \pm 1.0$	$0.3^{+1.2}_{-0.2}$	$5.7^{+4.1}_{-2.7}$	$1.9 \pm 1.1$
$1.6 \pm 0.3$	$3.2^{+2.5}_{-1.9}$	$2.1 \pm 1.0$	$0.3^{+1.2}_{-0.2}$	$7.2^{+5.0}_{-3.4}$	$1.9 \pm 1.1$
$1.1 \pm 0.2$	$2.2^{+1.7}_{-1.3}$	$2.1 \pm 1.0$	$0.3^{+1.2}_{-0.2}$	$5.7^{+4.1}_{-2.7}$	$1.9 \pm 1.1$

# Dynamical evolution I

- **Neutron stars are born in star-forming regions**, i.e., in the Galactic disk along the Milky Way's spiral arms, **and receive kicks** during the supernova explosions.
- We make the following assumptions:
  - Electron-density model (Yao et al., 2017) + rigid rotation with  $T = 250$  Myr.
  - Exponential disk with scale height  $h_c = 0.18$  kpc (Wainscoat et al., 1992).
  - Single-component Maxwell kick-velocity distribution with dispersion  $\sigma_k = 265$  km/s (Hobbs et al., 2005).
  - Galactic potential (Marchetti et al., 2019).

Artistic illustration of the Milky Way (credit: NASA JPL)



$$\mathcal{P}(z) = \frac{1}{h_c} e^{-\frac{|z|}{h_c}}$$

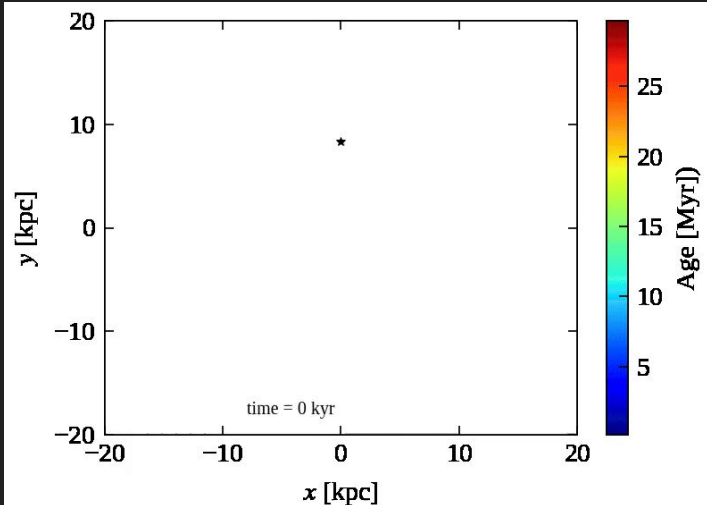
$$\mathcal{P}(v_k) = \sqrt{\frac{2}{\pi}} \frac{v_k^2}{\sigma_k^3} e^{-\frac{v_k^2}{2\sigma_k^2}}$$

# Dynamical evolution II

- For our Galactic model  $\Phi_{\text{MW}}$ , we evolve the stars' position & velocity by **solving Newtonian equations of motion** in cylindrical galactocentric coordinates:

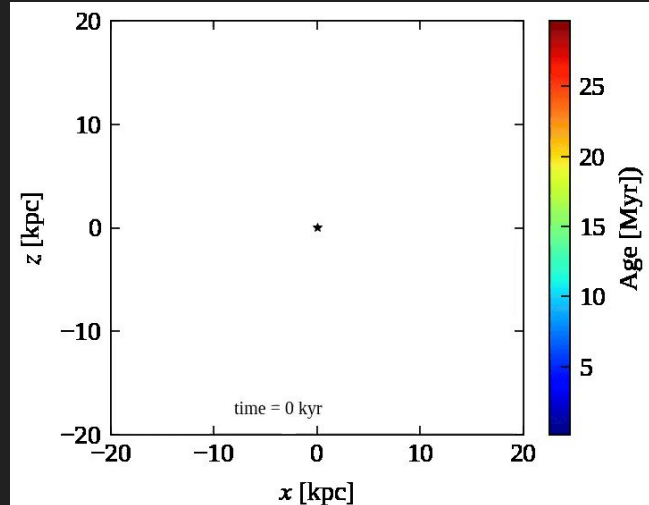
$$\ddot{\vec{r}} = -\vec{\nabla}\Phi_{\text{MW}}$$

Top view



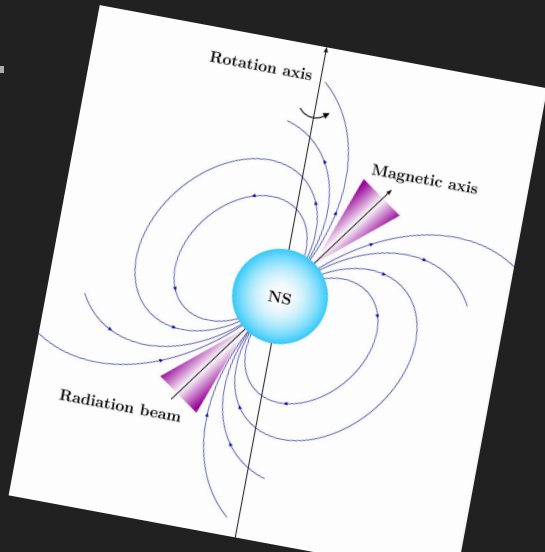
Galactic evolution tracks  
for  $h_c = 0.18$  kpc,  
 $\sigma = 265$  km/s.

Side view



# Magneto-rotational evolution I

- The neutron-star magnetosphere exerts a torque onto the star. This causes spin-down and alignment of the magnetic and rotation axes.
- Neutron star **magnetic fields decay** due to the Hall effect and Ohmic dissipation in the outer stellar layer (crust) (e.g., Viganó et al., 2013 & 2021).
- We make the following assumptions:
  - Initial periods follow a log-normal with  $\mu_P$  and  $\sigma_P$  (Igoshev et al., 2022)
  - Initial fields follow a log-normal with  $\mu_B$  and  $\sigma_B$  (Gullón et al., 2014)
  - Above  $\tau \sim 10^6$  yr, field decay follows a power-law with  $B(t) \sim B_0 (1 + t/\tau)^\alpha$ .



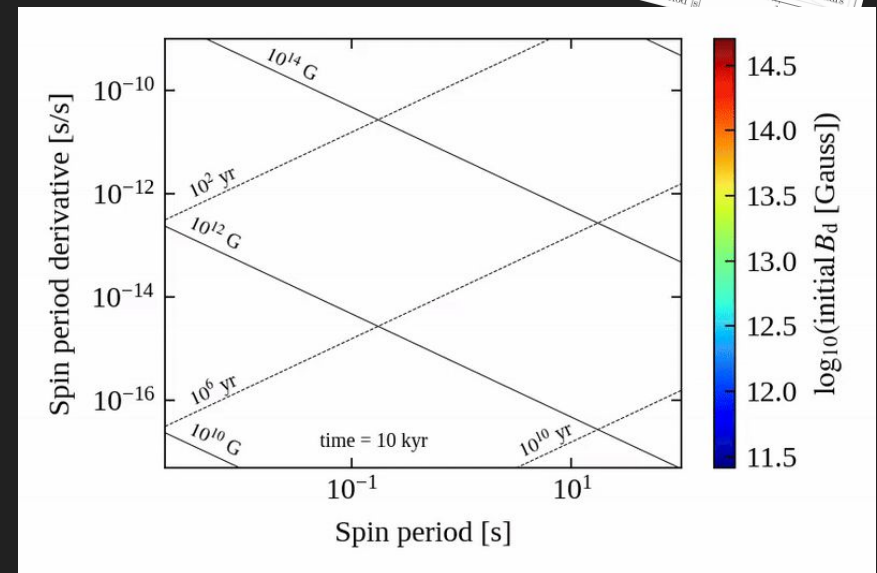
$$\mathcal{P}(\log P_0) = \frac{1}{\sqrt{2\pi}\sigma_P} \exp\left(-\frac{[\log P_0 - \mu_P]^2}{2\sigma_P^2}\right)$$

Here, we **vary** the five uncertain parameters  $\mu_P$ ,  $\mu_B$ ,  $\sigma_P$ ,  $\sigma_B$  and  $\alpha$ .

# Magneto-rotational evolution II

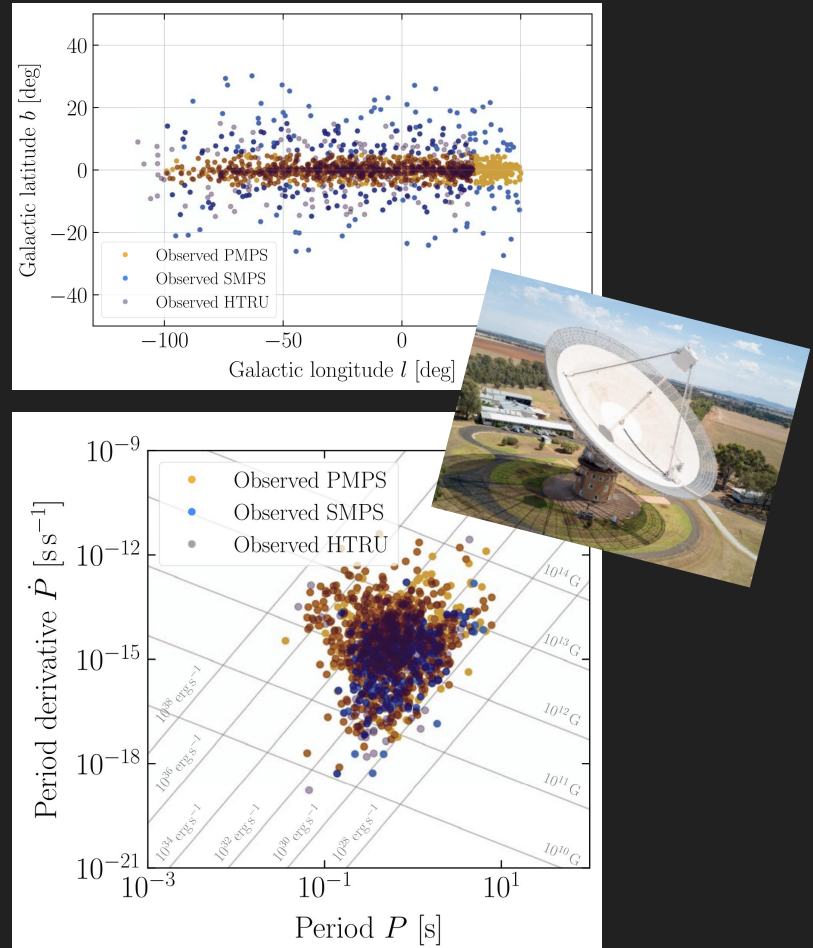
- To model the magneto-rotational evolution, we numerically solve two coupled ordinary differential equations for the period and the misalignment angle (Aguilera et al., 2008; Philippov et al. 2014).
- We use results from 2D magneto-thermal simulations to determine the evolution of the magnetic field below  $10^6$  yr (Viganò et al. 2021).
- This allows us to follow the stars'  $P$  and  $\dot{P}$  evolution in the  $P\dot{P}$ -plane.

$\dot{P}$  evolution tracks for  
 $\mu_P = -0.6$ ,  $\sigma_P = 0.3$ ,  $\mu_B = 13.25$  and  $\sigma_B = 0.75$ .



# Three pulsar surveys

- After modelling the pulsars' brightness in radio, we count them as detected if they surpass a certain threshold.
- We then compare our simulated populations with three surveys from Murriyang (the Parkes Radio Telescope):
  - Parkes Multibeam Pulsar Survey (PMPS): 1,009 PSRs
  - Swinburne Parkes Multibeam Pulsar Survey (SMPS): 278 PSRs
  - High Time Resolution Universe Survey (HTRU): 1,023 PSRs

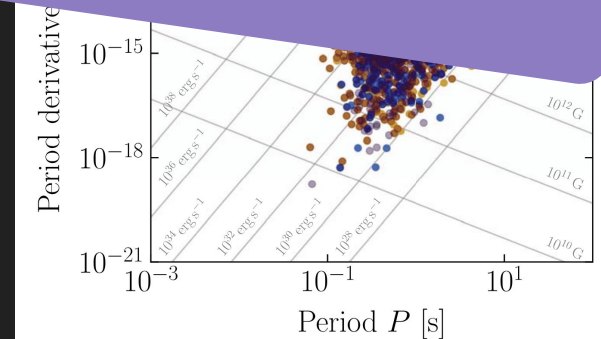
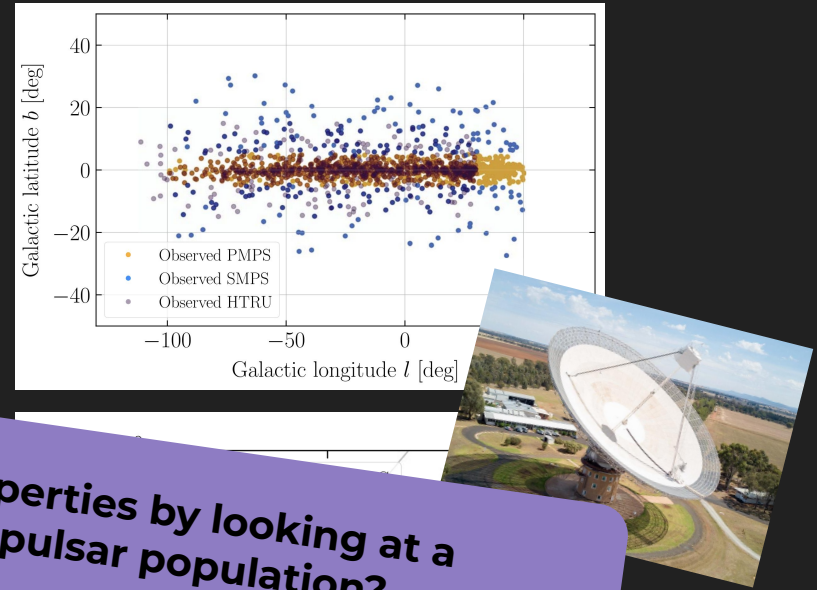


# Three pulsar surveys

- After modelling the pulsars' brightness in radio, we count them as detected if they surpass a certain threshold.
- We then compare the pulsar populations from the Parkes Multibeam Pulsar Survey (PMPS), the Swinburne Parkes Multibeam Pulsar Survey (SMPS) and the High Time Resolution Universe Survey (HTRU).

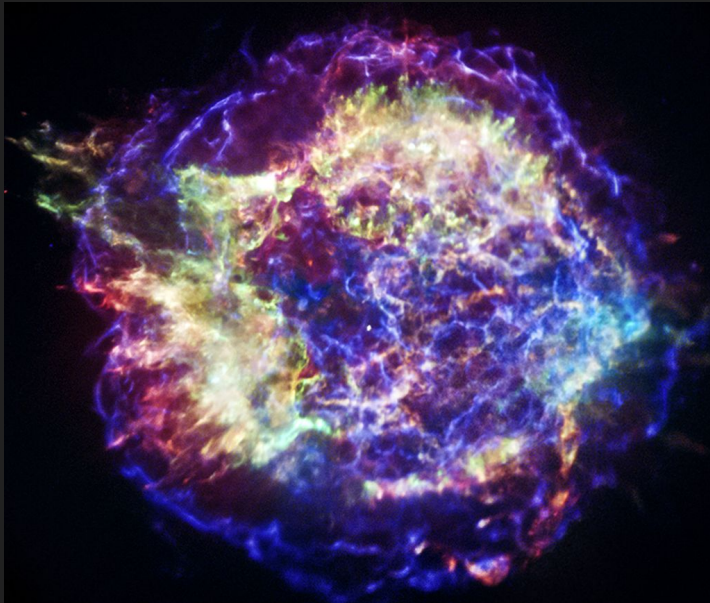
Can we constrain birth properties by looking at a current snapshot of the pulsar population?

- Parkes Multibeam Pulsar Survey (PMPS): 1,009 PSRs
- Swinburne Parkes Multibeam Pulsar Survey (SMPS): 218 PSRs
- High Time Resolution Universe Survey (HTRU): 1,023 PSRs



# Outline

- Radio Astronomy
- ML and Radio Astronomy
- Neutron Stars
- SBI for Pulsar Populations
- Summary



Cassiopeia A supernova remnant  
(credit: NASA/CXC/SAO)



## Comparing models and data

- Comparing observations to models and **constraining regions of the parameter space** that are **most probable given the data** is fundamental to many fields of science.
- Pulsar population synthesis is complex and has **many free parameters**. To compare synthetic simulations with observations, people have
  - Randomly sampled and then optimised ‘by eye’ (e.g., Gonthier et al., 2007)
  - Compared distributions of individual parameters using  $\chi^2$ - and KS-tests (e.g., Narayan & Ostriker, 1990; Faucher-Giguère & Kaspi, 2006)
  - Used annealing methods for optimisation (Gullón et al., 2014)
  - Performed Bayesian inference for simplified models (Cieślar et al., 2020)

These methods do not scale well and are **difficult to use** with the **multi-dimensional data** produced in population synthesis.

# Statistical inference

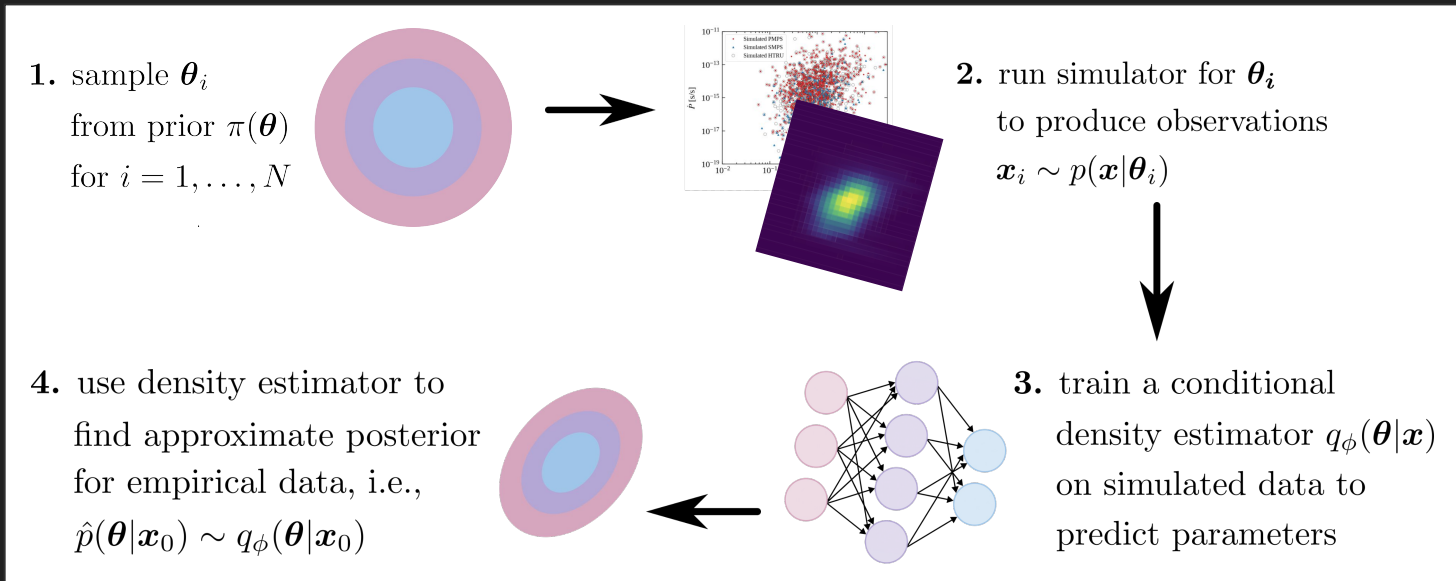
- To obtain probable regions of parameter spaces that explain our data (i.e., we do not need exact point estimates), we perform statistical inference.
- This is where **Bayesian inference** comes in: based on some prior knowledge  $\pi(\theta)$ , a stochastic model and some observation  $x$ , we want to infer the most likely distribution  $P(\theta|x)$  for our model parameters  $\theta$  given the data  $x$ . This is **encoded in Bayes' Theorem**:

$$\underbrace{P(\theta|x)}_{\text{posterior}} = \frac{\overbrace{P(\theta)}^{\text{prior } \pi} \overbrace{P(x|\theta)}^{\text{likelihood } \mathcal{L}}}{\underbrace{P(x)}_{\text{evidence}}}$$

For complex simulators, the **likelihood is defined implicitly and often intractable**. This is overcome with **simulation-based** (likelihood-free) **inference** (see e.g. Cranmer et al., 2020).

# Simulation-based inference I

- To perform **Bayesian inference for any kind of (stochastic) forward model** (e.g. those specified by simulators), we use the following approach:



# Simulation-based inference II

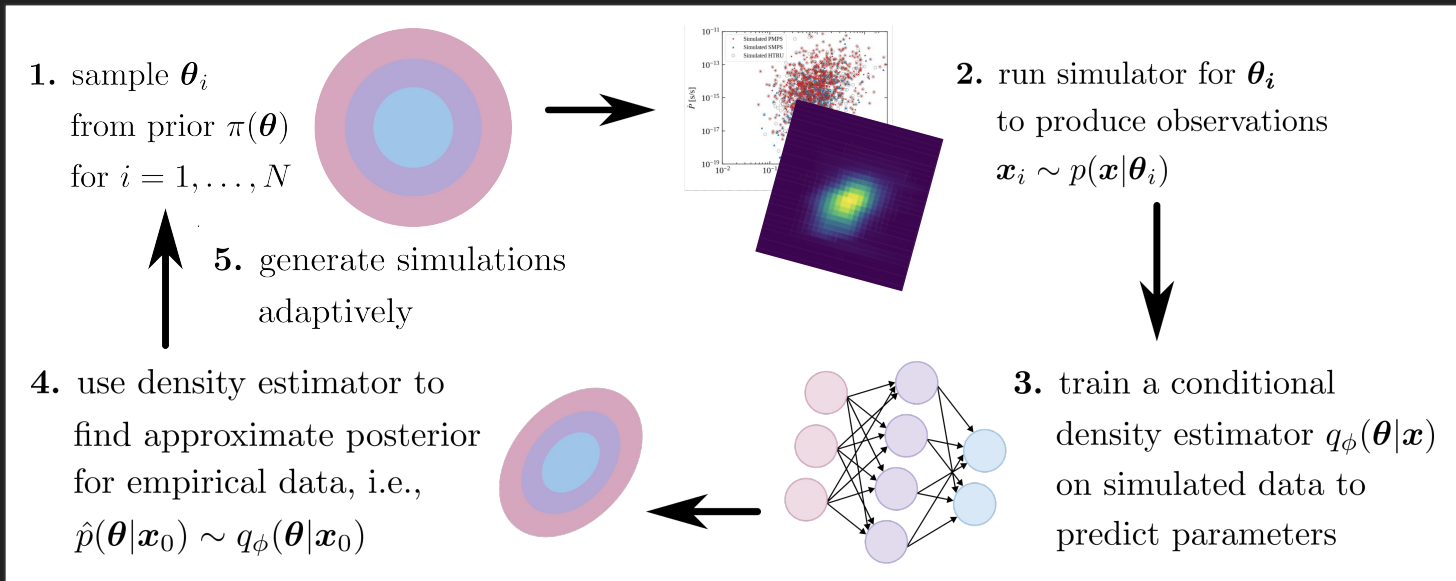
- Different approaches (all relying on deep learning) exist to **learn a probabilistic association** between the simulated data and the underlying parameters. These algorithms essentially focus on different pieces of Bayes' theorem:
  - Neural Posterior Estimation (NPE) (e.g., Papamakarios & Murray, 2016)
  - Neural Likelihood Estimation (NLE) (e.g., Papamakarios et al., 2019)
  - Neural Ratio Estimation (NRE) (e.g., Hermans et al., 2020; Delaunoy et al., 2022)

**We focus on NPE.** This allows us to **directly learn the posterior distribution**. In contrast, NLE and NRE need an extra (potentially time consuming) MCMC sampling step to construct a posterior.

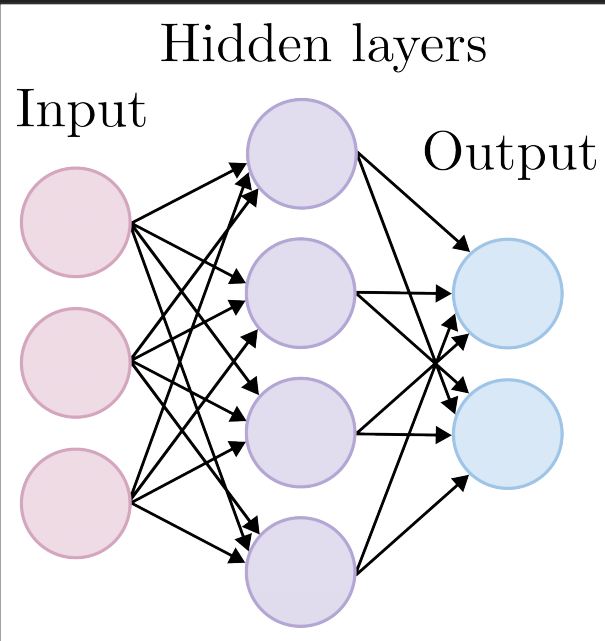
- All methods exist in sequential form (SNPE, SNLE, SNRE), which adds a fifth step to workflow. Instead of sampling from the prior, we adaptively generate simulations from the posterior. This typically requires fewer simulations.

# Simulation-based inference II

- To perform **Bayesian inference for any kind of (stochastic) forward model** (e.g. those specified by simulators), we use the following approach:



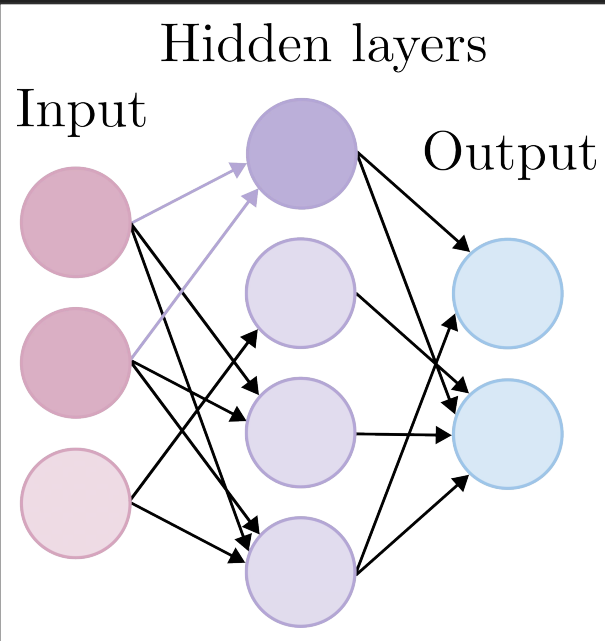
# Neural networks (NNs)



Sketch of a very simple  
fully connected neural network.

- A neural network is composed of layers, which represent stacks of neurons (objects holding a single numerical value). Each layer encodes a simplified representation of the input data.
- A deep-learning algorithm learns more and more about the input as the data is passed through successive hidden network layers.
- The Multilayer Perceptron is the simplest set-up where input and output are fully connected. In a convolutional NN, not all nodes are connected, which reduces the number of trainable parameters and allows more flexibility for training.

# Neural networks (NNs)



Sketch of a very simple convolutional neural network.

- A neural network is composed of layers, which represent stacks of neurons (objects holding a single numerical value). Each layer encodes a simplified representation of the input data.
- A deep-learning algorithm learns more and more about the input as the data is passed through successive hidden network layers.
- The Multilayer Perceptron is the simplest set-up where input and output are fully connected. In a convolutional NN, not all nodes are connected, which reduces the number of trainable parameters and allows more flexibility for training

# Convolutional and max pooling layers

- Besides fully connected layers, CNNs are composed of two types of filters:

## Convolutional filters



$$\begin{bmatrix} -1 & -1 & -1 \\ -1 & 8 & -1 \\ -1 & -1 & -1 \end{bmatrix}$$



## Max-pooling layers

3	1	0	9
8	4	7	3
6	5	0	4
1	2	9	0

$2 \times 2$

8	9
6	9

These filters recognise features, such as detecting edges of an object in an image.

These filters extract the most relevant features, helping to speed up the training process.

# SBI for radio pulsars

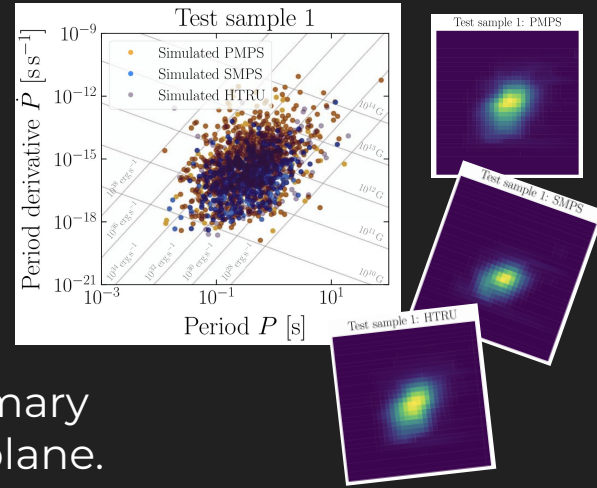
- With our complex population synthesis simulator, we fix the dynamics to a fiducial model and focus on the magneto-rotational evolution.
- From our simulated populations, we generate summary statistics: density maps for three surveys in the  $\dot{P}$ -plane.
- Build on PyTorch package sbi (Tejero-Cantero et al., 2020):

Varying the five parameters  $\mu_p$ ,  $\mu_B$ ,  $\sigma_p$ ,  $\sigma_B$  and  $\alpha$ , we simulate 360,000 synthetic pulsar populations over 6 weeks.

$$\begin{aligned}\mu_{\log B} &\in \mathcal{U}(12, 14), \\ \sigma_{\log B} &\in \mathcal{U}(0.1, 1), \\ \mu_{\log P} &\in \mathcal{U}(-1.5, -0.3), \\ \sigma_{\log P} &\in \mathcal{U}(0.1, 1), \\ a_{\text{late}} &\in \mathcal{U}(-3, -0.5).\end{aligned}$$

# SBI for radio pulsars

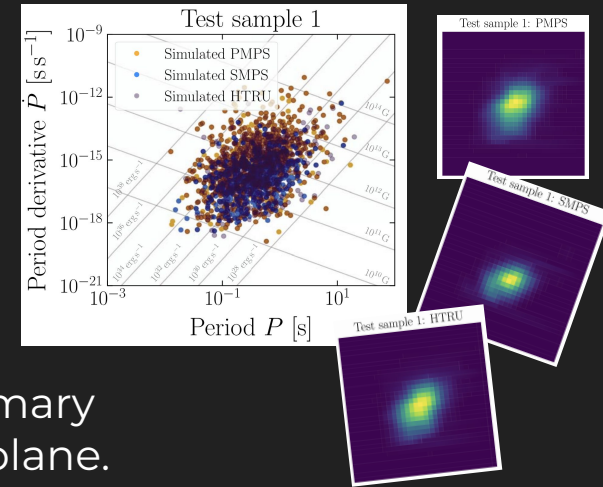
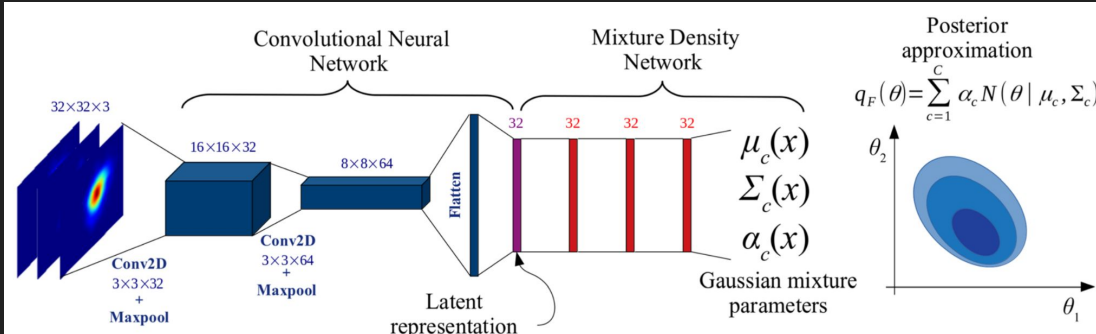
- With our complex population synthesis simulator, we fix the dynamics to a fiducial model and focus on the magneto-rotational evolution.
- From our simulated populations, we generate summary statistics: density maps for three surveys in the  $\dot{P}$ - $P$ -plane.
- Build on PyTorch package sbi (Tejero-Cantero et al., 2020):



$$\begin{aligned}\mu_{\log B} &\in \mathcal{U}(12, 14), \\ \sigma_{\log B} &\in \mathcal{U}(0.1, 1), \\ \mu_{\log P} &\in \mathcal{U}(-1.5, -0.3), \\ \sigma_{\log P} &\in \mathcal{U}(0.1, 1), \\ a_{\text{late}} &\in \mathcal{U}(-3, -0.5).\end{aligned}$$

# SBI for radio pulsars

- With our complex population synthesis simulator, we fix the dynamics to a fiducial model and focus on the magneto-rotational evolution.
- From our simulated populations, we generate summary statistics: density maps for three surveys in the  $\dot{P}$ -plane.
- Build on PyTorch package sbi (Tejero-Cantero et al., 2020):



$$\begin{aligned}\mu_{\log B} &\in \mathcal{U}(12, 14), \\ \sigma_{\log B} &\in \mathcal{U}(0.1, 1), \\ \mu_{\log P} &\in \mathcal{U}(-1.5, -0.3), \\ \sigma_{\log P} &\in \mathcal{U}(0.1, 1), \\ a_{\text{late}} &\in \mathcal{U}(-3, -0.5).\end{aligned}$$

# Posterior results

- We use an ensemble of networks to infer on the observed population:

$$\mu_{\log B} = 13.10^{+0.08}_{-0.10},$$

$$\sigma_{\log B} = 0.45^{+0.05}_{-0.05},$$

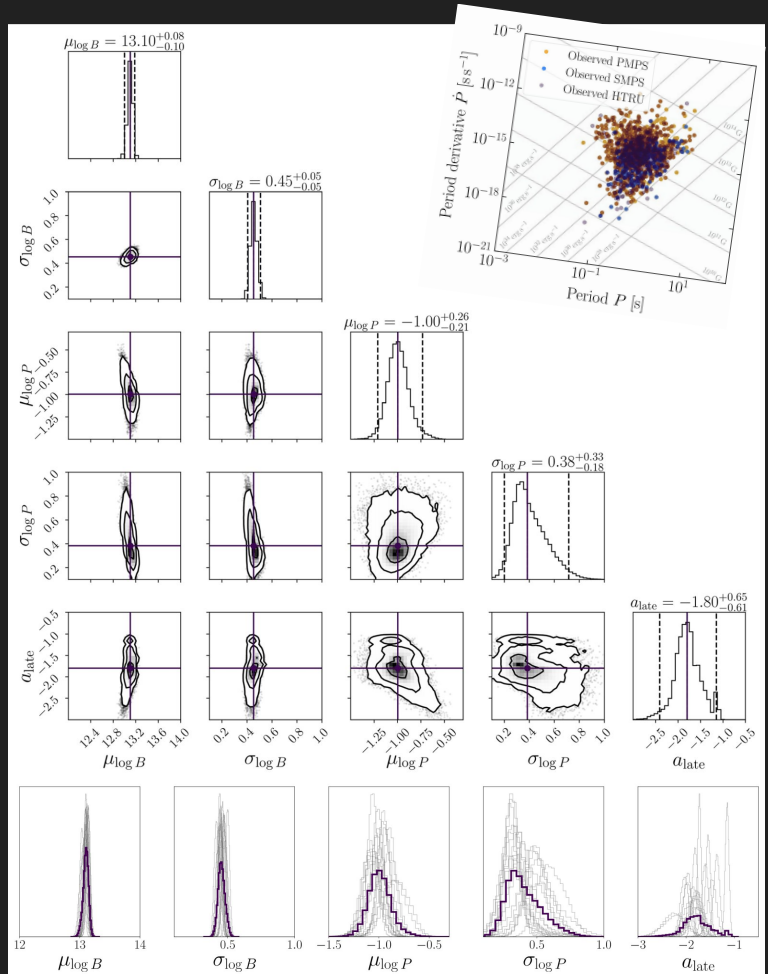
Graber et al. (2024)

$$\mu_{\log P} = -1.00^{+0.26}_{-0.21},$$

$$\sigma_{\log P} = 0.38^{+0.33}_{-0.18},$$

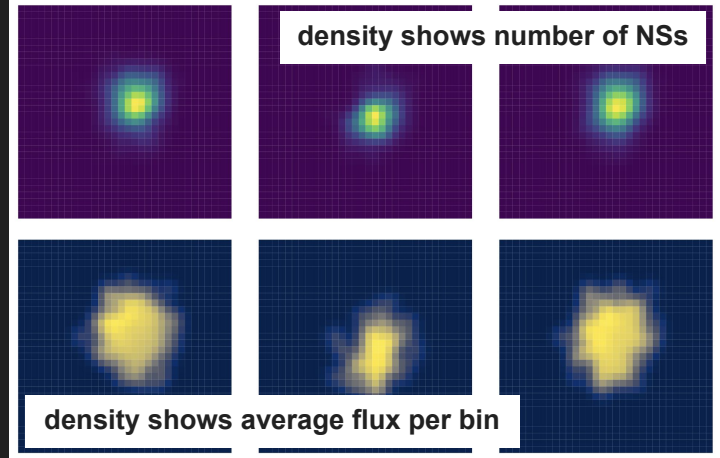
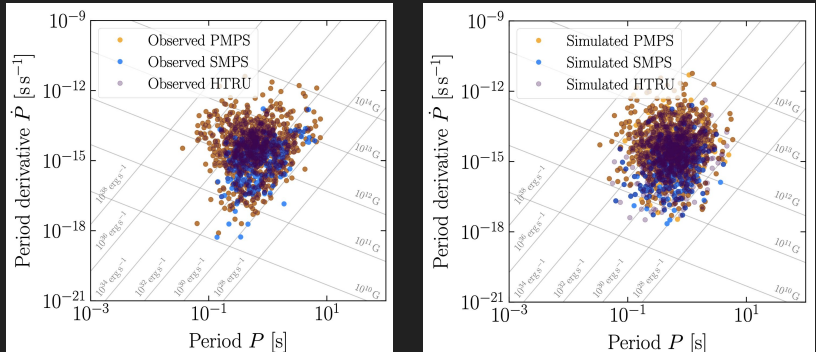
$$a_{\text{late}} = -1.80^{+0.65}_{-0.61}.$$

- Initial B-field parameters are narrower than initial P posteriors (expected due to degeneracies).
- Posteriors for late-time evolution do not overlap causing bimodality (hinting at missing info/physics).



# Sequential SBI for radio pulsars

- We have now implemented a sequential workflow (Deistler et al. 2022) that iteratively produces simulations as needed.
- This method plus adding radio flux information allows us to infer 7 parameters with only 10,000 simulations in a few days.



$$\begin{aligned}\mu_{\log B} &= 13.09^{+0.20}_{-0.14}, \\ \sigma_{\log B} &= 0.50^{+0.04}_{-0.04}, \\ \mu_{\log P} &= -0.67^{+0.33}_{-0.53}, \\ \sigma_{\log P} &= 0.55^{+0.22}_{-0.27},\end{aligned}$$

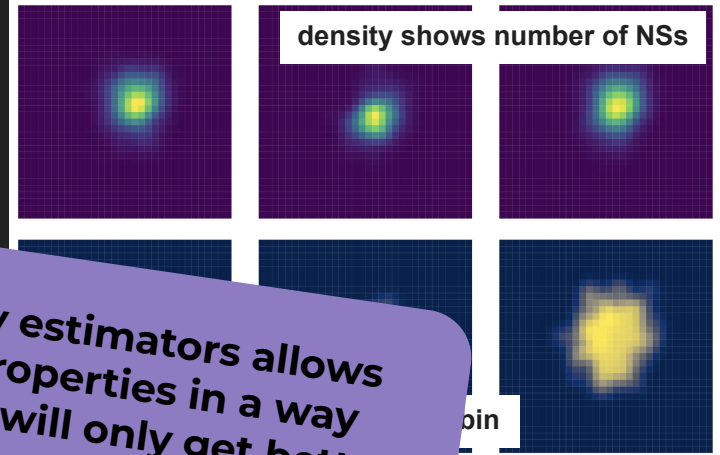
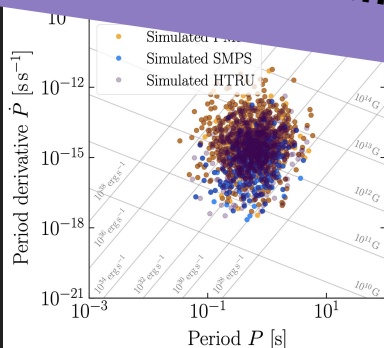
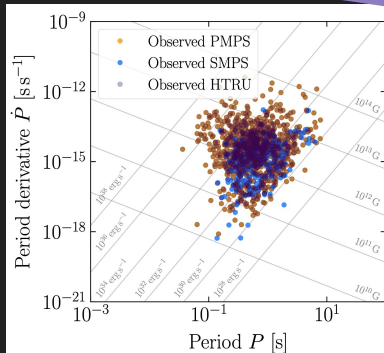
Pardo et al. (2025)

$$\begin{aligned}a_{\text{late}} &= -0.88^{+0.16}_{-0.17}, \\ \mu_{\log L_0} &= 26.17^{+0.19}_{-0.16}, \\ \alpha &= 0.68^{+0.10}_{-0.07}.\end{aligned}$$

# Sequential SBI for radio pulsars

- We have now implemented a sequential workflow (Deistler et al. 2022) that iteratively produces simulations as needed.
- This means we can make predictions with our model.

*Using neural networks as density estimators allows us to learn about neutron star properties in a way that has never been possible. This will only get better as SKAO will observe many more radio pulsars.*



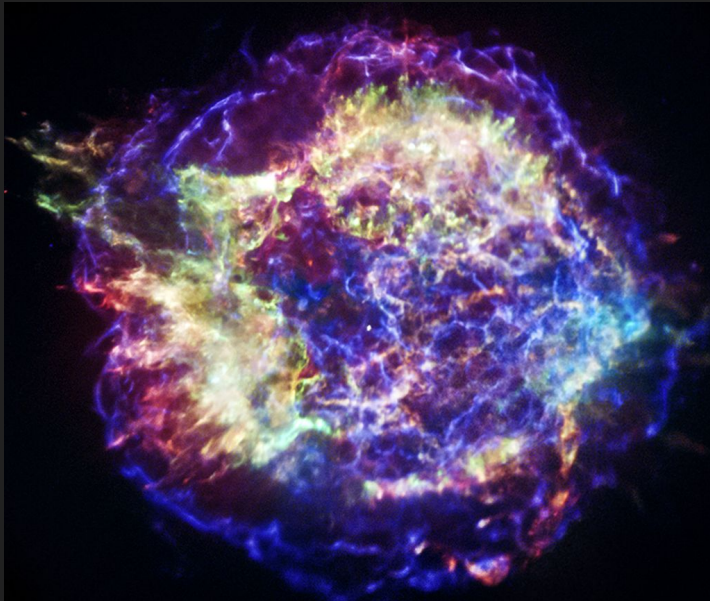
$$\begin{aligned}\mu_{\log B} &= 13.09_{-0.14}, \\ \sigma_{\log B} &= 0.50_{-0.04}, \\ \mu_{\log P} &= -0.67_{-0.53}, \\ \sigma_{\log P} &= 0.55_{-0.27},\end{aligned}$$

$$\begin{aligned}a_{\text{late}} &= -0.88_{-0.17}^{+0.16}, \\ \mu_{\log L_0} &= 26.17_{-0.16}^{+0.19}, \\ \alpha &= 0.68_{-0.07}^{+0.10}.\end{aligned}$$

Deistler et al. (2025)

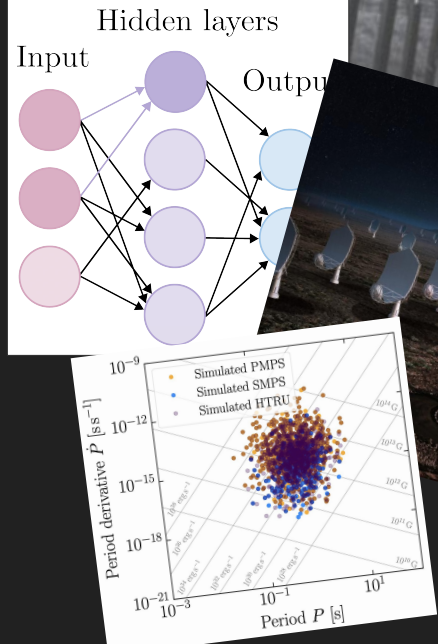
# Outline

- **Radio Astronomy**
- **ML and Radio Astronomy**
- **Neutron Stars**
- **SBI for Pulsar Populations**
- **Summary**



Cassiopeia A supernova remnant  
(credit: NASA/CXC/SAO)

# Summary



- Radio astronomy allows a unique view into astrophysical phenomena otherwise hidden from view.

- Key challenges in radio astronomy (RFI, large data volumes) can lend themselves to be solved by ML algorithms.

- Simulators in astronomy are very complex, making standard Bayesian inference often impossible.

- Using flexible neural networks to estimate posteriors is an exciting new way to learn about unknown astrophysics.